Journal of Hazardous Materials 466 (2024) 133589

Contents lists available at ScienceDirect

Journal of Hazardous Materials

journal homepage: www.elsevier.com/locate/jhazmat

Research Article

Impact of polyamide microplastics on riparian sediment structures and Cd (II) adsorption: A comparison of natural exposure, dry-wet cycles, and freeze-thaw cycles

Si Liu [a,b], Jinhui Huang [a,b,*], Wenjuan He [a,b], Lixiu Shi [c], Wei Zhang [a,b], Enjie Li [a,b], Chenyu Zhang [a,b], Haoliang Pang [a,b]

[a] College of Environmental Science and Engineering, Hunan University, Changsha 410082, PR China
[b] Key Laboratory of Environmental Biology and Pollution Control (Hunan University), Ministry of Education, Changsha 410082, PR China
[c] College of Hydraulic and Environmental Engineering, Changsha University of Science and Technology, Changsha 410114, PR China

HIGHLIGHTS

- Macro-aggregate and aggregate stability significantly reduced by combined FT cycles and MPs.
- DW and FT cycles showed an obvious increase in sediment properties.
- The aromaticity and humification degree of DOM were significantly decreased in 10% MPs-treated sediment.
- DW and FT cycles slightly increased the Cd(II) adsorption onto 0.1% and 1% MPs-treated sediments.
- There was a relationship between aggregate stability and sediment organic carbon.

GRAPHICAL ABSTRACT

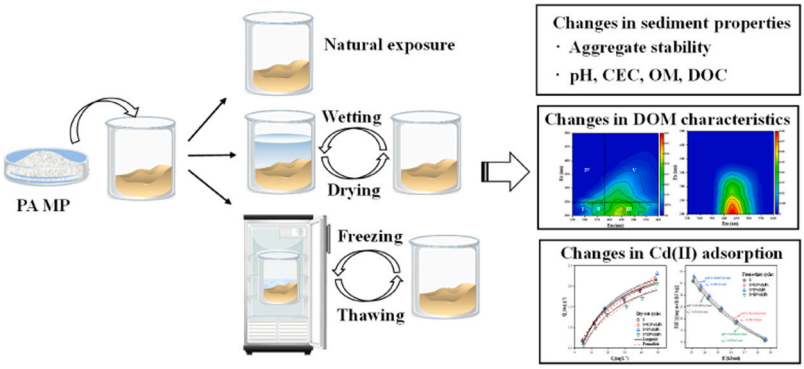

ARTICLE INFO

Keywords:
Microplastics
Riparian sediment
Hydrological processes
Dissolved organic matter
Adsorption

ABSTRACT

Microplastics (MPs) accumulation in sediments has posed a huge threat to freshwater ecosystems. However, it is still unclear the effect of MPs on riparian sediment structures and contaminant adsorption under different hydrological processes. In this study, three concentrations of polyamide (PA) MPs-treated sediments (0.1%, 1%, and 10%, w/w) were subjected to natural (NA) exposure, dry-wet (DW) cycles, and freeze-thaw (FT) cycles. The results indicated that PA MPs-added sediment increased the micro-aggregates by 10.1%−18.6% after FT cycles, leading to a decrease in aggregate stability. The pH, OM, and DOC of sediments were significantly increased in DW and FT treatments. In addition, the increasing concentration of PA MPs showed an obvious decrease in aromaticity, humification, and molecular weight of sediment DOM in FT treatments. Also, high level of MPs was more likely to inhibit the formation of humic-like substances and tryptophan-like proteins. For DW and FT cycles, 0.1% and 1% PA MPs-treated sediments slightly increased the adsorption capacity of Cd(II), which may be ascribed to the aging of MPs. Further correlation analysis found that DW and FT altered the link between DOM

* Corresponding author at: College of Environmental Science and Engineering, Hunan University, Changsha 410082, PR China.
E-mail addresses: huangjinhui@hnu.edu.cn, huangjinhui_59@163.com (J. Huang).

https://doi.org/10.1016/j.jhazmat.2024.133589
Received 27 October 2023; Received in revised form 10 January 2024; Accepted 19 January 2024
Available online 21 January 2024

indicators, and aggregate stability was directly related to the changes in sediment organic carbon. Our findings revealed the ecological risk of MPs accumulating in riparian sediments under typical hydrological processes.

1. Introduction

Microplastics (MPs, plastic particles ≤5 mm in diameter) are of great interest as emerging pollutants and have been found in land, river, ocean, and atmospheric environments [1]. Particularly, more than 90% of MPs will ultimately sink into sediments after entering the river environment, which may be related to microbial colonization, heterogeneous aggregation, and gravity-driven deposition [2]. The riparian ecosystem usually serves as a buffer zone to receive various pollutants including heavy metals, antibiotics, and MPs [3]. Among them, municipal sewage and stormwater runoff input large amounts of MPs into the riparian sediment. Owing to recalcitrant to degradation and stability under poor light and anoxic conditions, MPs would inevitably participate in sediment processes and interfere with sediment structure [4]. Therefore, studying the potential effects of MPs in riparian sediments is conducive to better understanding the environmental behavior of MPs.

The riparian zones are generally considered to be highly dynamic ecosystems under the influence of seasonal weather conditions [5]. Dry-wet (DW) cycles and freeze-thaw (FT) cycles are the typical features of riparian sediments [6,7]. Additionally, the sediment aggregates of the riparian zone generally determine sediment structure and properties and potentially impact sediment ecosystem functions. DW and FT cycles are both significantly interfered with the stability of sediment aggregates. Wang et al. [8] found that FT cycles promoted the breakage of soil macroaggregates into microaggregates, leading to an increase in soil specific surface area. Nsabimana et al. [9] reported that continuous DW cycles improved the soil aggregate stability and increased the mean volume diameter by 14.25%. At the same time, the variations in sediment aggregates would indirectly affect the internal properties (e.g., pH, organic matter). However, considering the large number of MPs detected in riparian sediments worldwide, few studies are exploring the effects of MPs on riparian sediment structure under different hydrological processes.

Dissolved organic matter (DOM) is the most active substrate of sediment, which affects the biogeochemical cycle and ecological function of river ecosystems [10]. Moreover, DOM is also critical for regulating sediment carbon balance and contaminant behavior [11]. However, plastic polymers are mainly composed of carbon-based chains, they may potentially leach DOM into the aquatic environment, thus forming a new carbon source and altering the existing carbon cycle process [12]. Our previous study found that low level of MPs addition (0.05% and 0.5%, w/w) significantly decreased the dissolved organic carbon (DOC) concentration and facilitated DOM decomposition [13]. Sun et al. [14] reported that polyethylene (PE) and polystyrene (PS) MPs (1% w/w) had no effect on the DOC content but promoted the formation of aromatic-like compounds in soil DOM. Considering the high diversity and heterogeneity of DOM in riparian sediment, the structural characteristics of DOM are also often affected by changes in hydrological processes. For instance, the DW process could promote the degradation of labile fractions and retain aromaticity and molecular weight fractions of DOM [15]. Therefore, the response of sediment DOM to MPs under different hydrological processes is still worthy of further exploration.

The variations in soil structure affected by the MPs will interfere with the adsorption of contamination in soils. In particular, heavy metals are considered to be the common contamination in soil and sediment [16,17]. Li et al. [18] found that the adsorption capacity of MPs to Pb(II) was decreased with increasing concentration of MPs, which may be attributed to the occupation of adsorption sites by MPs in sediments. Additionally, Chen et al. [19] also concluded that the presence of MPs (0.5 wt %) in soil decreased Pb(II) sorption. The possible reason is that the MPs addition reduced the proportion of macroaggregates and the stability of aggregates. At the same time, DW and FT processes may influence the environmental behavior of heavy metals by altering the soil properties. It has been reported that the adsorption amount of Cd(II) to freeze-thaw treated soils was significantly decreased [20]. However, under the background of a specific hydrological process, changes in the adsorption performance and mechanism of heavy metals in sediments induced by MPs have not been studied.

Polyamide (PA), which is mainly used as ropes for seine nets and fishing, is one of the most highly detected types of MPs in sediments [21]. Sun et al. [22] reported that the PA MPs promoted the abundance of genes related to the C and N cycle, which affected the soil microbial diversity. Therefore, in this study, we aim to explore the effect of three riparian hydrological processes on sediment properties and Cd(II) adsorption in the presence of PA MPs. Therefore, under the conditions of natural exposure, dry-wet cycles, and freeze-thaw cycles, the objectives of this study were as follows: (1) to investigate the impact of different concentrations of PA MPs on the variation of sediment basic properties and aggregate stability; (2) to probe the effects of MPs addition on the composition and structure of sediment DOM; (3) to compare the adsorption capacity and mechanism of Cd(II) onto sediment spiked with MPs; (4) to clarify the link between sediment structures under different hydrological processes. This study will provide new insights for evaluating the ecological risks of MPs in riparian sediments subjected to different hydrological processes.

2. Materials and methods

2.1. Sediment and microplastic

The sediment used in this study was sampled from the riparian zone of Xiangjiang River (one of the important tributaries of the Yangtze River), Hunan Province, China. Sediment samples were air-dried, and then ground to pass through a 2 mm mesh sieve. The basic properties of the sediment were exhibited in Table S1 in the Supporting Information.

The virgin PA MP (density: 1.15 g/cm^3, size: 150 μm) was brought from Zhongcheng Plastic Co. Ltd, China. The microstructure and element distribution of PA MP were observed using Scanning Electron Microscopy (SEM, Sigma 300, Germany) and Energy Dispersive Spectroscopy (EDS, Smartedx, Germany) (Fig. S1a). The surface of functional groups of PA MP was determined using Fourier transform infrared spectrometry (FTIR, Thermo Scientific Nicolet iN10, USA) (Fig. S1b).

2.2. Incubation experiments

The microcosm experimental design of this study contained adding 0.1%, 1%, and 10% PA MP to sediment in MPs-spiked groups. The control group was performed without adding MPs. Fuller and Gautam [23] reported that the amount of MPs detected in soils ranged from 0.03%− 6.7% (w/w). Also, the 0.1% and 1% MPs concentrations were based on MPs doses commonly used in previous studies, which were considered to be relevant to real sediment environments. Besides, considering the variability of the actual sediment environment and better comparison of the effects of different concentrations of MPs on sediment properties, we selected 10% concentration to simulate the extreme conditions in heavily polluted areas [13]. In addition, a total of 100 g riparian sediment amended with MPs was placed in the 500 mL beaker. Each group was kept at 70% of water holding capacity (WHC) and exposed for 7d to activate the microbial communities [15]. Next, simulation of natural (NA) exposure, DW cycles, and FT cycles was conducted in this study. The NA exposure as compared was set and

incubated for 30 d in the climatic incubator with dark and room temperature (25 ℃), and sediment samples were kept the humidity at 70% (v/w). For each DW cycle, sediment samples were incubated with two conditions involved wetting (topsoil kept 2 cm water layer for 12 h) and drying (dried at 40 ℃ in an oven for 12 h) [24]. For each FT cycle, sediment samples with 70% WHC were frozen at − 20 ℃ in a refrigerator for 12 h and then thawed at 25 ℃ for 12 h [25]. The DW and FT cycles were repeated 30 times. In total, 36 treatment groups were designed with three replicates per group.

2.3. Physicochemical analysis of sediment

The size distribution of sediment aggregates was determined by the wet-sieving method [26], including large macro-aggregates (LMA, >2000 μm), small macro-aggregates (SMA, 2000–250 μm), micro-aggregates (MI, 250–53 μm), and silt + clay fractions (SC, <53 μm). The sieving procedures were displayed in Text S1. Additionally, the aggregate index of mean weight diameter (MWD) for each group was calculated as follows:

$$MWD = \sum_{i=1}^{n} x_i y_i \quad (1)$$

where x_i is the average diameter of the aggregate size (mm), and y_i is the weight proportion of aggregate size i.

The pH of sediment-water slurry (1:5, w/v) was measured using a pH meter (ST2100, Ohaus, Changzhou, China). Sediment cation exchange capacity (CEC) was determined after extraction with barium chloride solution. Sediment organic matter (OM) was analyzed based on the potassium dichromate volumetric method. Sediment DOM concentration was expressed as the DOC concentration, which was assayed with the total organic carbon (TOC) analyzer (TOC-V CPH, Shimadzu, Japan).

2.4. Spectral analysis

The ultraviolet-visible (UV-Vis) spectra of DOM samples were determined by the UV-Vis spectrophotometer (UV-2550, Shimadzu, Japan) with a 10 mm quartz cuvette. The wavelength was scanned in the range of 200–700 nm with a scan interval of 1 nm. The specific absorbance at 254 and 280 nm divided by the DOC concentration of the sample ($SUVA_{254}$ and $SUVA_{280}$) was defined as the indicators of aromaticity and humification of DOM, respectively [27]. Moreover, the E_2/E_3 was calculated as absorbance at 254 nm divided by absorbance at 365 nm, which was generally negatively correlated with the molecular weight of DOM [28].

The fluorescence excitation-emission matrix (EEM) spectra of the DOM samples were measured using a fluorescence spectrometer (F-7000, Hitachi, Japan). The excitation (Ex) and emission (Em) wavelengths were set to 200–500 nm (5 nm increments) and 250–600 nm (5 nm increments), respectively. The scan speed for the spectra was 12,000 nm/min. In addition, fluorescence regional integration (FRI) was used to quantitatively analyze fluorescence intensities in the wavelength region of EEM spectra [29]. The components and relative fluorescence intensities of DOM samples were also analyzed coupled with parallel factor analysis (PARAFAC) modeling using MATLAB2020b (Math Works, MA, USA). More details were shown in Text S2.

2.5. Adsorption experiments

The adsorption isotherms of Cd(II) by CK and MPs-treated sediment samples were conducted. In brief, the stock solution of Cd(II) (100 mg L^{-1}) was prepared by dissolving $Cd(NO_3)_2$ in Milli-Q water. The diluted solutions containing different initial concentrations of Cd(II) (10, 20, 30, 40, 50, and 60 mg L^{-1}) were carried out by 8 g L^{-1} of adsorbents. The background solution contained 0.1 M $CaCl_2$ to maintain ionic strength. The solution pH was adjusted to 6 using 0.1 M NaOH or 0.1 M HNO_3. Then, the mixed solutions were shaken at 150 rpm in a thermostatic shaker with dark and 25 ℃ for 24 h. The solutions were collected and filtered through 0.45 μm membrane filter. The Cd(II) concentration was measured by Flame Atomic Absorption Spectrophotometer (FAAS, PinAAcle900F, China). Also, the FTIR spectra after adsorption and site energy distribution analysis were performed to further clarify the adsorption mechanism of Cd(II) onto sediments. The detailed adsorption models and site energy distribution theory were depicted in Text S3.

3. Results and discussion

3.1. Changes in sediment aggregate size distribution and stability

As shown in Table 1, the proportion of SMA was dominant among sediment aggregates accounting for 48.33%− 69.54% in all treatments, while the proportion of LMA was almost negligible. In NA exposure treatments, the addition of 0.1% and 1% PA MPs reduced the MI by 13.3% and 20.8%, while the proportion of SMA and SC correspondingly increased. In contrast, higher contents of MI and SC were found in the 10% PA MPs treatment (32.08% and 5.86%, respectively). Once MPs enter the sediment surface, they will incorporate into the sediment matrix and interfere with the sediment aggregate structure [19]. The above results indicated that low level of PA MPs as an extra binding agent favored the association of the existing aggregates with soil components (e.g., minerals) to produce new small macro-aggregates or smaller aggregates [30]. However, higher levels of PA MPs exhibited strong hydrophobicity and reduced soil bulk density, thus leading to the formation of micro-aggregates (< 250 μm) and a decrease in aggregate stability [31]. Another possible reason is that higher concentrations of PA MPs introduced more fracture points during the aging process, which may prevent smaller aggregates from integrating into macro-aggregates [32]. Similarly, de Souza Machado et al. [31] found that the soil aggregate stability decreased with increasing MPs concentration.

Meanwhile, the DW and FT cycles during incubation without adding MPs significantly increased the percentage of SC. And the MWD value decreased by 3.9% and 11.4%, respectively, which indicated that DW and FT cycles destabilized the riparian sediment aggregates. In general, repeated DW and FT cycles may generate differential swelling and shrinking forces within the aggregates, resulting in the weakening of the binding force among particles inside the aggregates [33,34]. The addition of PA MPs showed no significant influence on sediment aggregates' size distribution and stability after DW cycles. The possible reason is that MPs may incorporate into aggregates and promote the formation of the new reorganized aggregate, thus improving the resistance of particles inside the aggregates to the DW cycles [35]. However, the FT cycles significantly increase the proportion of MI and SC in the MPs-treated sediment. Specifically, the addition of 0.1%, 1%, and 10% PA MPs increased the micro-aggregates (<250 μm) by 10.1%, 12.2%, and 18.6%, respectively, which may be related to the variation of soil water content at FT cycles [36]. de Souza Machado et al. [31] found that the increasing concentration of MPs enhanced the water holding capacity of soil. When the water content was higher, the expansion force of ice crystals inside the aggregate increased, thus aggravating the destruction of the sediment aggregates [37].

3.2. Changes in physicochemical properties of sediment

As shown in Fig. 1a, the sediment pH affected by 0.1% and 1% PA MPs exhibited an evident increase in the NA exposure, while significantly decreased in 10% PA MPs-treated sediments. This can be explained by the aging and degradation of PA MPs, leading to the release of chemical compounds into the sediment and thus affecting sediment pH [38]. In addition, the released chemical compounds may indirectly affect sediment pH by altering sediment bacterial communities. Zhang et al. [39] found that the presence of 1% MPs increased soil pH, which

Table 1
Changes in size distribution and stability of aggregates.

Treatments	MPs concentration	LMA (%)	SMA (%)	MI (%)	SC (%)	MWD (mm)
NA	0	0.58 ± 0.155 bc	65.16 ± 3.53 ab	29.66 ± 0.90 bcd	4.60 ± 1.38c	0.79 ± 0.041 ab
	0.1%	0.64 ± 0.202 ab	68.36 ± 5.24 a	25.71 ± 2.66 cd	5.29 ± 0.33c	0.82 ± 0.059 a
	1%	0.34 ± 0.043c	69.54 ± 4.18 a	23.50 ± 1.29 d	6.61 ± 0.30 bc	0.83 ± 0.044 a
	10%	0.42 ± 0.091 bc	61.64 ± 3.66 ab	32.08 ± 2.10 abcd	5.86 ± 1.36 bc	0.75 ± 0.037 ab
DW	0	0.90 ± 0.267 a	62.10 ± 0.62 ab	26.68 ± 2.48 cd	10.32 ± 1.36 ab	0.76 ± 0.073 ab
	0.1%	0.31 ± 0.113c	62.37 ± 4.19 ab	28.60 ± 3.31 bcd	8.71 ± 1.83 abc	0.76 ± 0.045 ab
	1%	0.58 ± 0.002 bc	63.77 ± 0.13 ab	27.61 ± 0.31 bcd	7.04 ± 0.44 bc	0.77 0.002 ab
	10%	0.39 ± 0.001 bc	61.45 ± 0.50 ab	30.74 ± 1.42 bcd	7.42 ± 0.49 abc	0.75 ± 0.003 ab
FT	0	0.30 ± 0.002c	56.61 ± 0.64 bc	35.00 ± 2.04 abc	8.10 ± 1.41 abc	0.70 ± 0.005 bc
	0.1%	0.48 ± 0.078 bc	52.08 ± 2.31c	36.78 ± 1.92 ab	10.66 ± 0.32 ab	0.66 ± 0.021c
	1%	0.49 ± 0.048 bc	51.16 ± 4.07c	36.17 ± 2.55 ab	12.18 ± 1.35 a	0.65 ± 0.042c
	10%	0.57 ± 0.056 bc	48.33 ± 0.18c	40.92 ± 0.86 a	10.18 ± 0.99 ab	0.62 ± 0.002c

Note: LMA (large macroaggregates, > 2 mm); SMA (small macroaggregates, 0.25 ~ 2 mm); MI (microaggregates, 0.053 ~ 0.25 mm); SC (silt + clay, < 0.053 mm); MWD (mean weight diameter). Different lowercase letters show significant differences ($p < 0.05$).

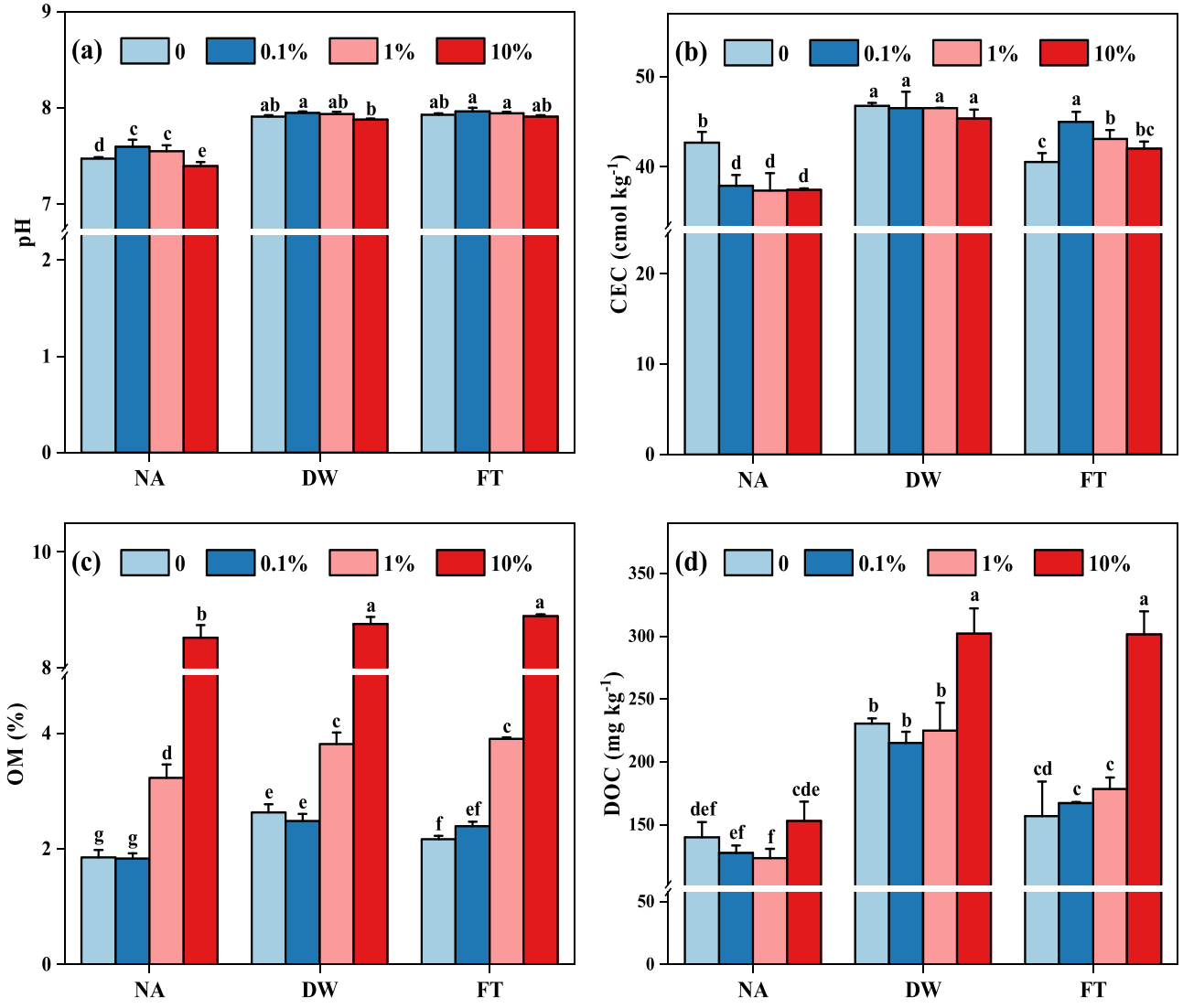

Fig. 1. pH (a), cation exchange capacity (CEC, b), organic matter (OM, c), dissolved organic matter (DOC, d) of sediments from different treatments. Different lowercase letters mean significant differences ($p < 0.05$) among treatments.

may be attributed to the changes in microbial activity. After DW and FT cycles, the pH significantly increased in sediments without adding MPs, which may be attributed to the consumption of protons due to the enhanced microbial activity [40]. However, the pH was closer to the control group in the presence of PA MPs in DW and FT treatments. This may be because DW and FT cycles could alleviate the effects of chemical compounds released by MPs on sediment pH. Moreover, the MPs significantly reduced the sediment CEC by 11.2%– 12.4% after NA exposure (Fig. 1b). The original aggregate structure was disrupted by the addition of MPs, thus resulting in the decrease of sediment colloid to

adsorb cations [41]. The CEC of all treatments showed a significant increase after DW cycles, whereas the MPs did not exert any apparent variation on CEC. In contrast, for the FT cycles, adding different concentrations of MPs elevated the CEC of sediment. One possible reason is that FT cycles cause water redistribution of sediment and MPs incorporated into aggregates provide a reactive surface to alter cation exchange [42].

Compared to the NA exposure group, the content of sediment OM and DOC were both significantly increased in the DW and FT groups (Fig. 1c, d). Especially in the absence of MPs, the concentration of OM and DOC in sediments after DW cycles increased by 1.42 and 1.65 times, respectively. The possible explanation is that the destruction and reorganization of the sediment aggregates caused by DW and FT cycles facilitated the release of organic matter [43]. In all treatments, the addition of 1% and 10% PA MPs resulted in 1.7–4.6 times increase in sediment OM content, while there was no significant effect in 0.1% MPs-treated sediment. On the one hand, MPs will be directly imported into sediments as a main carbon source. Also, natural sediment OM was adsorbed by the porous structure of MPs [44]. On the other hand, MPs would stimulate specific microbial metabolism and enzyme activity, which may promote the decomposition and transformation of sediment OM [45]. Noteworthy, DOM was more sensitive to the variation in sediment conditions than OM [46]. For the NA exposure, adding 0.1% and 1% PA MPs decreased the DOC content by 8.9% and 11.9%, respectively, and the 10% MPs addition instead increased it by 9.4%. The results were consistent with the findings of our previous study [13]. However, only the 10% PA MPs-treated group showed a significant increase in DOC content after DW and FT cycles, indicating that high levels of MPs are more likely to bind to aggregates and release dissolved organic carbon during DW and FT cycles.

3.3. Impact on DOM characteristics of sediment

3.3.1. Changes in DOM chemical properties of sediment

The chemical properties of sediment DOM were shown in Table 2. In the NA exposure, the $SUVA_{254}$ and $SUVA_{280}$ were obviously increased by the addition of 0.1% and 1% MPs, while 10% MPs addition slightly decreased. The possible reason is that low level of MPs increased the condensation degree of DOM structure, thus promoting the formation of aromatic compounds [47]. The decrease of E_2/E_3 ratio was observed in MPs-treated sediment, which may be attributed to the small molecular weight of DOM was more conducive to the conversion into large one affected by MPs [47]. Additionally, the level of $SUVA_{254}$ and $SUVA_{280}$ after DW and FT cycles were increased without adding MPs, suggesting that the aromatic and hydrophobic fractions of DOM could be preserved and formed under the DW and FT conditions. However, the increasing concentration of PA MPs reduced the value of $SUVA_{254}$ and $SUVA_{280}$ after DW and FT cycles. Specifically, 10% MPs addition significantly decreased the $SUVA_{254}$ and $SUVA_{280}$ by 34.8% and 54.2% in DW treatments, and by 36.4% and 56.6% in FT treatments, respectively. It might be because the presence of MPs facilitated sediment microbes to utilize refractory DOM and transform it into labile DOM under the action of external forces [15]. Furthermore, the E_2/E_3 ratio was significantly increased by 1.4–1.9 times with increasing concentration of MPs after FT cycles. Decreased in aromaticity, humification, and molecular weight of DOM in FT treatments may result from the biodegradation of DOM induced by MPs and FT [48].

3.3.2. Changes in DOM fluorescence components of sediment

Fluorescence EEMs of DOM in sediment were compared for different PA MP concentrations (Fig. 2). A strong fluorescence peak was observed at region III in all treatments, which was related to fulvic acid-like matter. The fluorescence intensity of this peak varied with the concentration of PA MPs. For the NA exposure and DW cycles, the intensity enhanced with the addition of 0.1% and 1% PA MPs, while decreased in the 10% MPs-treated sediment. In addition, the intensity decreased with increasing MPs concentration after FT cycles. Also, FT cycles resulted in a peak with higher fluorescence intensity in region IV, which was related to microbial by-product analogs. Area integration was employed to obtain the percentage of the volume of five regions (Fig. S2). Clearly, the highest contribution proportion in the sediment DOM was tryptophan-like protein (region II) and fulvic-like compounds (region III) in all treatments. The effect of PA MPs concentration exhibited no significant differences in the relative abundance of five regions. Interestingly, FT cycles significantly increased the relative abundance in region II, whereas it decreased in region III. It indicated that FT cycles facilitated the release of tryptophan-like protein and the immobilization of fulvic-like compounds [49,50].

Furthermore, the HIX, BIX, and FI were calculated based on fluorescence EEM spectra (Table 2). The HIX values after FT cycles were lower than that in other treatments, which was consistence with the changes of $SUVA_{254}$ and $SUVA_{280}$. In addition, FT and DW cycles significantly decreased the HIX in sediments amended with 10% PA MPs, suggesting that high level of MPs inhibited the humification of the sediment DOM. Compared to NA exposure, DW cycles significantly decreased the BIX value, which revealed that the biodegradation of DOM in DW treatments was at low level [51]. However, the BIX values were higher than 1 after FT cycles, which may be attributed to an increased contribution of microbial-derived organics. While for FI, the values in all treatments were higher than 1.9, indicating that the dominant source of DOM was microbial metabolism [52]. Besides, the addition of MPs showed no negligible change in BIX and FI values. It may mean microbial activity is relatively stable in response to MPs dose.

The sediment DOM in all treatments was divided into four fluorescent components based on the PARAFAC model (Fig. 3). Component 1 (C1) and Component 2 (C2) were identified as the humic-like compounds. C1 showed Ex/Em at 235/405 nm, which was derived from biological or microbial activity [53]. C2 was attributed to terrestrial humic-like components with Ex/Em at 255/495 nm [54]. Component 3 (C3, Ex/Em = 240/350) and Component 4 (C4, Ex/Em = 275/305) were

Table 2
Changes in UV-Vis spectra and fluorescent indexes of DOM in riparian sediment.

Treatments	MPs concentration	$SUVA_{254}$ ($L^{-1}\cdot mg\cdot m^{-1}$)	$SUVA_{280}$ ($L^{-1}\cdot mg\cdot m^{-1}$)	E_2/E_3	HIX	BIX	FI
NA	0	2.22 ± 0.23 abc	1.66 ± 0.19 abc	5.82 ± 1.00c	0.72 ± 0.02 ab	0.97 ± 0.02 b	2.16 ± 0.05 ab
	0.1%	2.64 ± 0.45 ab	2.03 ± 0.41 ab	4.46 ± 0.59c	0.70 ± 0.02 abc	1.00 ± 0.02 ab	2.14 ± 0.12 ab
	1%	2.87 ± 1.00 a	2.24 ± 0.86 a	4.41 ± 0.92c	0.70 ± 0.02 abc	0.97 ± 0.03 b	2.07 ± 0.01 ab
	10%	1.97 ± 0.59 bc	1.55 ± 0.50 abc	5.00 ± 1.51c	0.69 ± 0.03 abc	0.96 ± 0.04 b	2.14 ± 0.03 ab
DW	0	2.56 ± 0.57 ab	1.98 ± 0.11 ab	4.29 ± 0.74c	0.72 ± 0.01 ab	0.89 ± 0.05c	2.09 ± 0.06 ab
	0.1%	2.47 ± 0.22 abc	1.90 ± 0.19 abc	4.85 ± 0.16c	0.73 ± 0.02 a	0.86 ± 0.05c	2.05 ± 0.09 b
	1%	2.32 ± 0.19 abc	1.75 ± 0.16 abc	4.87 ± 0.41c	0.73 ± 0.02 a	0.88 ± 0.01c	2.07 ± 0.05 ab
	10%	1.67 ± 0.05 cd	1.26 ± 0.05 cd	4.38 ± 0.38c	0.67 ± 0.02c	0.89 ± 0.06c	2.13 ± 0.06 ab
FT	0	2.40 ± 0.25 abc	1.82 ± 0.20 abc	5.53 ± 0.76c	0.69 ± 0.02 abc	1.04 ± 0.02 a	2.16 ± 0.10 ab
	0.1%	2.18 ± 0.11 abc	1.62 ± 0.11 abc	7.95 ± 1.81 b	0.68 ± 0.02 bc	1.01 ± 0.02 ab	2.19 ± 0.02 ab
	1%	2.01 ± 0.09 bc	1.49 ± 0.08 bc	8.32 ± 1.52 b	0.69 ± 0.02 abc	1.00 ± 0.02 ab	2.10 ± 0.03 ab
	10%	1.10 ± 0.24 d	0.79 ± 0.24 d	10.50 ± 2.36 a	0.66 ± 0.02c	0.90 ± 0.03c	2.20 ± 0.14 a

Note: Different lowercase letters show significant differences ($p < 0.05$) among treatments.

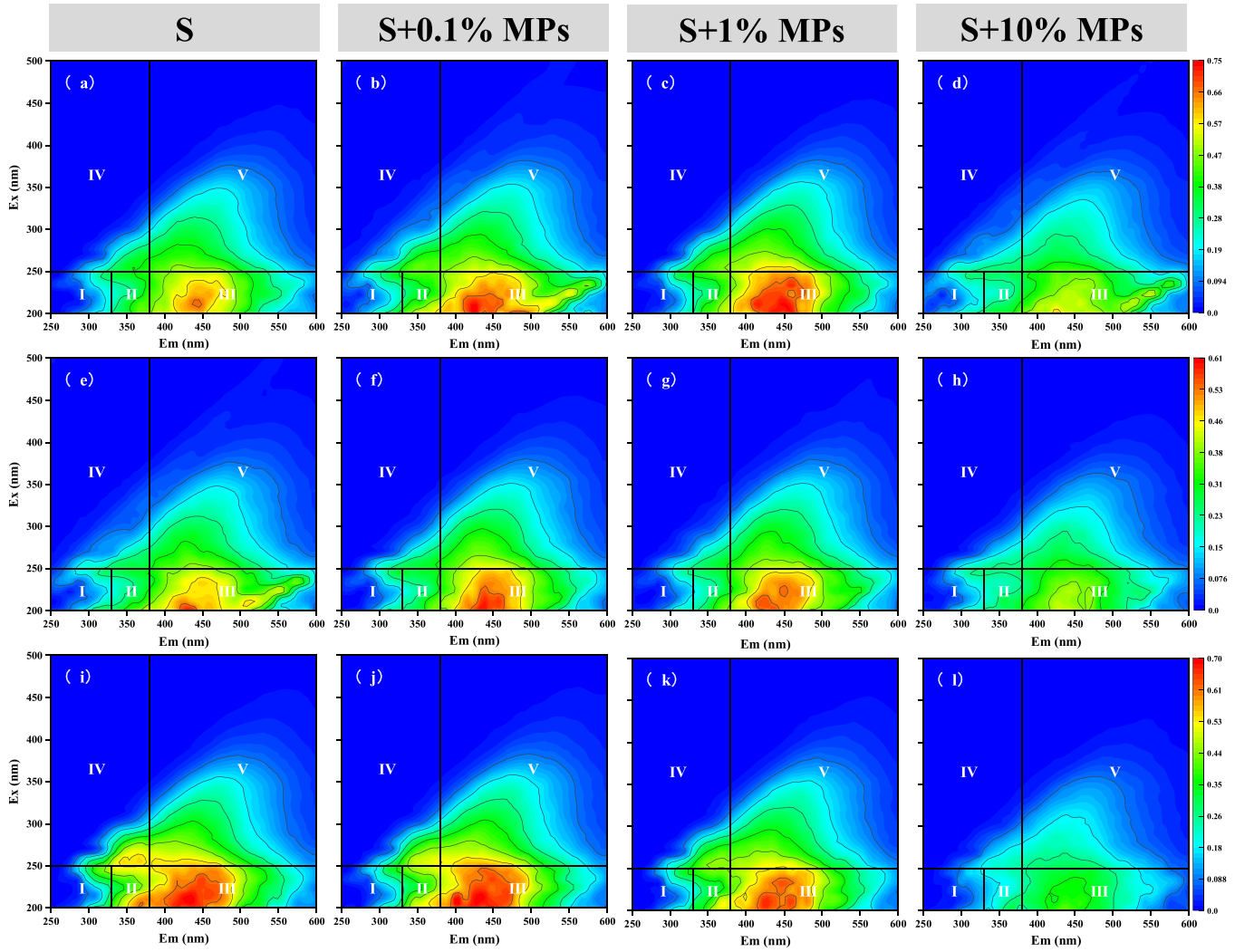

Fig. 2. Three-dimensional fluorescence spectra of sediment DOM in different treatments (NA exposure: a-d; DW cycles: e-h; FT cycles: i-l). Each 3D-EEM of sediment DOM was divided into five regions (region I: tyrosine-like protein; region II: tryptophan-like protein; region III: fulvic-like compounds; region IV: microbial by-product analogs; region V: humic acid substances).

characterized as tryptophan-like and tyrosine-like proteins, respectively [55,56]. Among them, the humic-like compounds accounted for higher amount in all treatments. Compared to the NA exposure, DW cycles significantly decreased the relative abundance of C1-C3. For example, humic-like fractions (C1 and C2) were reduced by 25.8% and 20.5%, and tryptophan-like protein was decreased by 35.5% without adding MPs, respectively. The results suggested that DW cycles could structurally disrupt the DOM organic carbon, thus facilitating the degradation of humic-like compounds and labile fractions in DOM. After FT cycles, the relative abundance of C2 in added 0.1% and 1% treatments significantly decreased, while C3 showed conversely trends. Due to the adaptation of cold-tolerant microorganisms to environmental changes, the low level of MPs may stimulate microbial activity to increase the proportion of labile DOM [7]. Besides, the relative abundances of C1 and C2 in 10% PA MPs-treated sediments were significantly decreased. Similarly, the relative abundance of C3 was also statistically lower in the 10% MPs addition. A possible explanation is that high level of MPs induced a ligand exchange with DOM, resulting in the fluorescence substances of DOM being covered [57]. Notably, the relative intensity of C4 was decreased after DW and FT cycles with the increasing concentration of MPs. On the one hand, tyrosine-like substances were usually derived from autochthonous production, and DW and FT cycles may alter the existing pattern [58]. On the other hand, MPs pollution inhibited microbial degradation to produce the aromatic protein [6].

3.4. Changes of Cd(II) adsorption in sediments

As shown in Fig. 4a-c, as well as the fitted data in Table S2, the adsorption isotherm of Cd(II) with all treatments were better fitted by the Freundlich model ($R^2 > 0.96$). This indicated that Cd(II) sorption onto sediments was a multilayer and heterogeneous adsorption process [59,60]. The adsorption amount of Cd(II) was lower in DW and FT treatments than that in the NA exposure, which may be ascribed to the destruction of sediment aggregates. As mentioned above, the micro-aggregates were increased after DW and FT cycles. However, the mineral components that play a key role in the adsorption of heavy metals mainly accumulate in macro-aggregates, thus leading to a decrease in the adsorption of heavy metals [60,61]. Besides, the adsorption amount of Cd(II) was decreased with increasing concentration of PA MPs after NA exposure. It could be observed that the K_F value was lower in the sediment-MPs mixture, suggesting that the presence of MPs could reduce the Cd-adsorbent interaction. PA MPs could be adsorbed on sediments through hydrophobic and electrostatic interactions. These interactions would occupy the adsorption sites of the sediments, thus reducing the adsorption of Cd(II) by the sediments [62]. A similar phenomenon was also observed in our previous study [13].

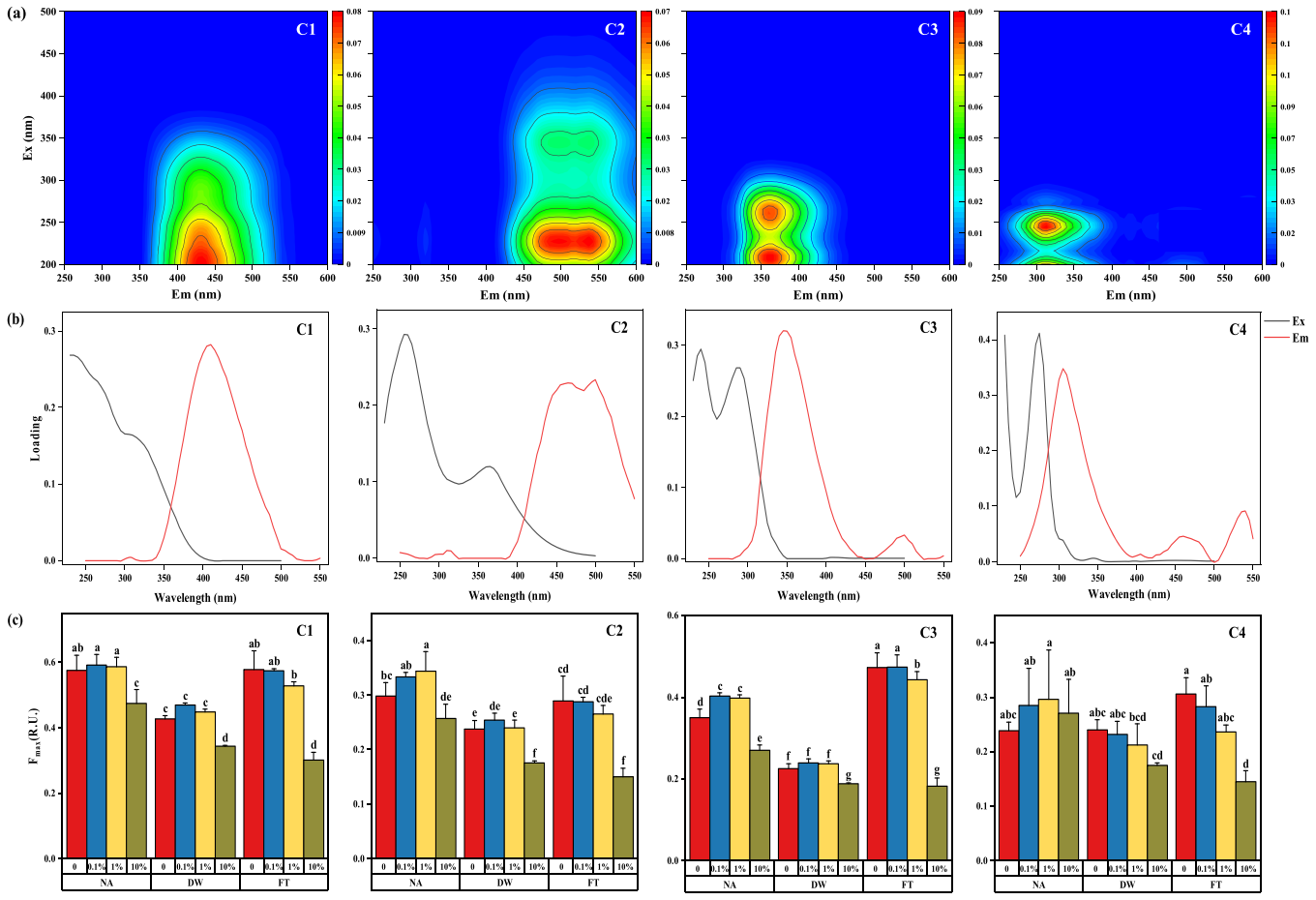

Fig. 3. (a) EEM contours plots of the four components; (b) Excitation/emission loadings of C1-C4; (c) The fluorescence intensity (F_{max}) of all treatments for each PARAFAC component. Different lowercase letters on the top of columns represent significant differences ($p < 0.05$).

After DW and FT cycles, the adsorption capacity of the sediments for Cd (II) slightly increased in the addition of 0.1% and 1% PA MPs, while decreased in 10% MPs-treated sediments. The reason may be that the surface properties of MPs were more prone to change when exposed to the DW and FT cycles, resulting in the enhanced adsorption capacity of Cd(II) by MPs [63]. However, the stronger disrupt effect on aggregates was observed in sediments amended with 10% PA MPs, which may lead to the decrease in Cd(II) adsorption by organic matter in sediment aggregates.

To further clarify the adsorption mechanisms of Cd(II) onto sediments, the FTIR spectrum and site energy distribution were employed. The 1% MPs-treated sediments were selected for FTIR analysis before and after adsorption (Fig. 5). Also, the variation of characteristic peaks was shown in Table S3. It was observed that DW and FT cycles did not change the adsorption peaks of the sediments, verifying that the physical disruption mainly occurred during this process. Besides, the characteristic adsorption peaks also had no obvious change after Cd(II) adsorption, except for the peaks located at 3697, 3620, 3439, and 1636 cm^{-1}. The peaks at 3697 and 3620 cm^{-1} showed a slight shifting after adsorption, which was related to the O−H stretching vibration of kaolinite [64]. Similarly, a slight shift of the peak at 1636 cm^{-1} was responsible for the C═O stretching of the carboxyl group [65]. These findings suggested that the oxygen-containing functional groups play a significant role in the Cd(II) adsorption process.

As shown in Fig. S3, site energy (E*) decreased gradually in all treatments as the amount of Cd(II) adsorbed onto sediments increased, verifying that the high-energy sorption sites were occupied by Cd ions firstly, followed by the low-energy sorption sites [66]. In the NA exposure, the average site energy (μ(E*)) decreased with the increasing concentration of PA MPs (Fig. 4d). This indicated that the presence of MPs would reduce the adsorption affinity between Cd(II) and sediments. The values of μ(E*) slightly increased after DW and FT cycles, revealing that the distribution range of adsorption sites expanded to the region with high energy (Fig. 4e, f). Also, due to the variations in sediment structures (e.g., sediment aggregate and OM as mentioned above), the surface site energy heterogeneity (σ_e^*) of sediments showed an increase. Generally, when the concentration of Cd(II) was high, the adsorption capacity of the sediment was stronger, and the adsorption process mainly occurred in the low-energy region [67]. The shift of the site distribution to the high-energy region further indicates that Cd ions were more mobile on the sediment surface. Noteworthy, it was observed that the values of μ(E*) and σ_e^* of the treatments after FT cycles were close. This may be because the internal adsorption sites of sediments were exposed and occupied by the MPs.

3.5. Correlation and analysis of the sediment properties

PCA was used to elucidate the DOM characteristics between the MPs-treated and control groups in different hydrological processes. As shown in Fig. 6a-c, the major principal components (PC1 and PC2) explained 89.5%, 95.8%, and 97.8% of the total variance, respectively. PC1 was highly positively correlated with C1, C2, C3, C4, $SUVA_{254}$, and $SUVA_{280}$, and negatively correlated with FI in different treatments. PC1 can be inferred as a factor related to the humic-like aromatic compounds and enrichment of proteins in samples [68]. 10% MPs addition exhibited relatively high negative PC1 scores in the three hydrological processes, which may be related to the strong effects of high levels of MPs on microbial metabolic activity. In the NA exposure, PC2 showed obvious

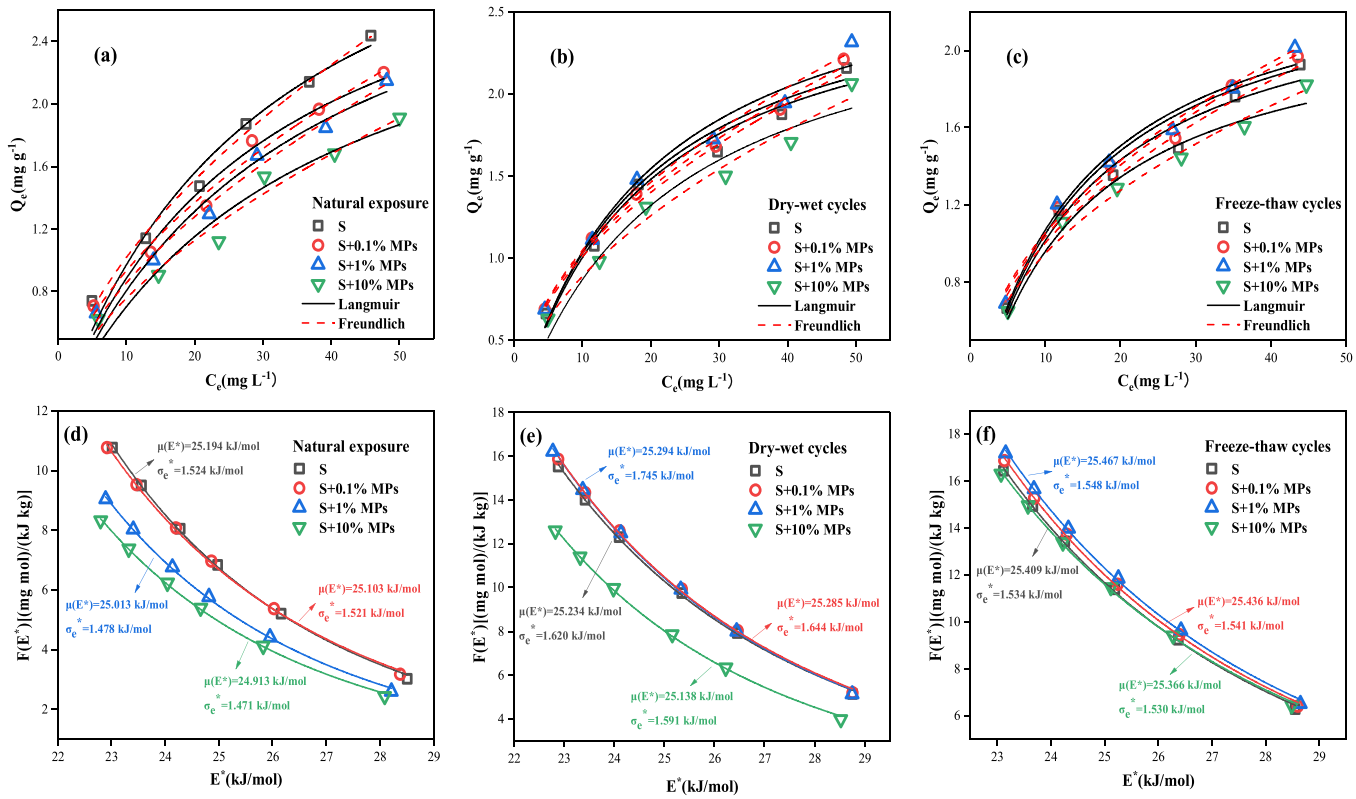

Fig. 4. Adsorption isotherms (a-c) and adsorption site energy distributions (d-f) of Cd(II) onto sediments among different treatments.

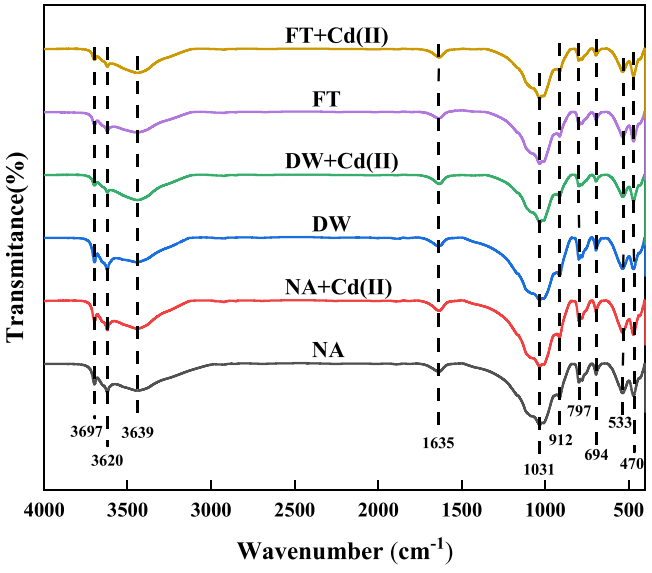

Fig. 5. FTIR spectra of 1% MPs-treated sediments in different conditions after adsorption of Cd(II).

positive loadings of HIX, and occurred higher scores in sediments without adding MPs, indicating that the addition of MPs could inhibit the sediment DOM humification. Additionally, DW and FT cycles reshaped the characteristics of DOM. After DW cycles, PC2 was associated with the high molecular weight substances and was related to the autochthonous DOM, as revealed by the positive loading of BIX and the negative loadings of E_2/E_3. Specially, MPs addition showed negative PC2 scores, possibly suggesting that MPs facilitated the biodegradation of the high molecular weight of DOM. In contrast, after FT cycles, FI was placed in the positive direction of PC2, while HIX was negatively paced on PC2. Noteworthy, 1% of MPs-treated sediment was located in regions with high negative PC2 scores, which may be ascribed to the increase of refractory substances in DOM [69].

The Pearson correlation further revealed the relationship between sediment properties and DOM parameters varied with the hydrological processes (Fig. 6d-e). For the NA exposure, the MWD was significantly correlated with the pH, $SUVA_{254}$, C2, and C3 positively and DOC concentration negatively. On the one hand, the presence of MPs may alter the intermolecular interaction of soil colloids which are sensitive to the pH changes, thus influencing the aggregation between sediment particles. On the other hand, disrupted sediment structure affected by MPs promoted the exposure of organic matter associated with minerals, which may change the release of DOC and the DOM humification process [47]. After DW cycles, it was observed that DOC was significantly positively correlated with FI and OM, while significantly negatively correlated with HIX, C1, C2, and C3. Due to the continuous alternating anoxic-oxic conditions change, microbial activity was boosted with the increasing concentration of organic carbon, thereby facilitating the decomposition of aromatic carbon into simple labile fractions [15]. However, other parameters had low prediction potency for MWD, indicating that the MPs addition acted as a physical protector of sediment organic carbon by resisting DW cycles damage to the sediment aggregates [70]. Additionally, the higher linear dependence between fluorescent components and optical indicators (i.e., $SUVA_{254}$, $SUVA_{280}$, HIX, and BIX) after FT cycles, which was consistent with the PCA result (Fig. 6c). Moreover, DOC showed a significant negative correlation with fluorescent components, $SUVA_{254}$, $SUVA_{280}$, and BIX. Because of the high-frequency FT cycles induced microorganisms to decompose sediment DOM and produce metabolites continuously, thus altering the humic structure of DOM [7]. Notably, a significant negative correlation was found between MWD and E_2/E_3. This result implied that sediment aggregates were broken into more micro-aggregates under the synergistic effect of FT and MPs, accompanied by the formation of more small molecular weight DOM.

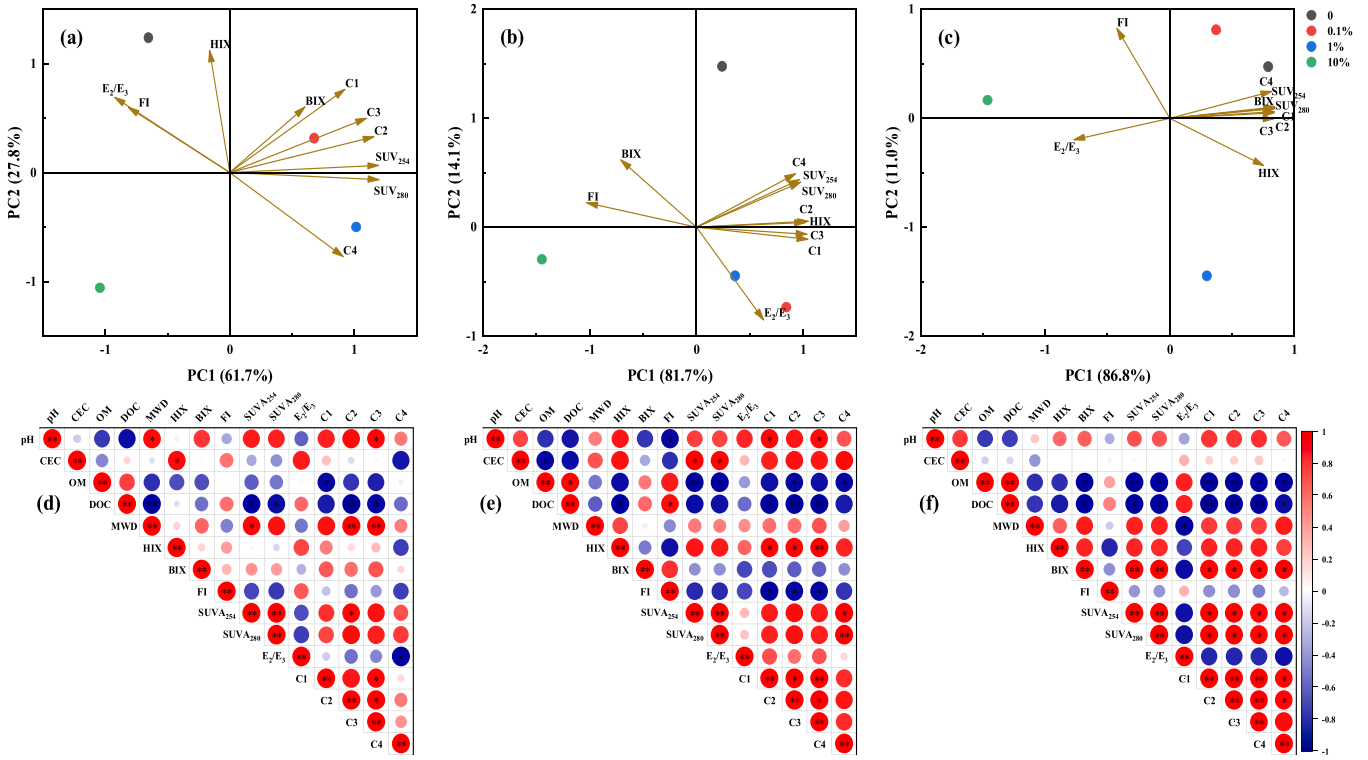

Fig. 6. Principal component analysis of DOM characteristics in different treatments (a-c); Pearson correlation analysis between sediment properties and DOM parameters (d-f). Note that: a,c: NA exposure; b,e: DW cycle; c, f: FT cycle.

4. Conclusion

In this study, we conducted a laboratory incubation to investigate the differences in the effects of different concentrations of PA MPs on sediment aggregate stability, sediment properties, and Cd(II) adsorption capacity under three hydrological processes. The results indicated that high levels of PA MPs decreased macro-aggregates and aggregate stability, and FT cycles significantly exacerbated sediment aggregate disruption. In addition, the pH, CEC, OM, and DOC of sediments were higher after DW and FT cycles, while MPs addition exhibited different effects on sediment properties. UV–vis and EEM results demonstrated that the changes in sediment DOM structures varied with PA MPs concentration and hydrological processes. Specifically, higher levels of MPs showed an obvious decrease in aromaticity and humification of sediment DOM in DW and FT treatments. Also, 10% MPs addition significantly altered sediment DOM composition by decreasing humic-like substances and tryptophan-like proteins. Furthermore, the adsorption capacity of Cd(II) onto sediment was affected by the DW and FT cycles. However, due to the competition of sediment adsorption sites, 10% of MPs-treated sediments of all treatments significantly reduced the Cd(II) adsorption. Simultaneous physical and chemical adsorption mechanisms dominated the adsorption of Cd(II) onto sediments. Principal component analysis indicated that MPs and sediment conditions showed synergetic effects on DOM characteristics. The correlation between the variations in MWD of sediment aggregates and DOM structure was also observed. In conclusion, this study will be beneficial for better understanding the impact of MPs accumulation on riparian sediment structure and contaminant transport under different hydrological processes. The impact of different MPs (types and degrees of aging) on the structure (water content and soil bulk density) and functions (carbon cycle and microbial community structure) of riparian sediments under different hydrological conditions requires further research.

CRediT authorship contribution statement

Liu Si: Data curation, Formal analysis, Investigation, Methodology, Software, Writing – original draft, Writing – review & editing. **Pang Haoliang:** Formal analysis, Resources. **Zhang Chenyu:** Methodology, Visualization. **Li Enjie:** Data curation, Investigation. **He Wenjuan:** Formal analysis, Investigation, Visualization. **Huang Jinhui:** Conceptualization, Funding acquisition, Supervision, Writing – review & editing. **Zhang Wei:** Software, Validation. **Shi Lixiu:** Project administration, Resources, Supervision.

Environmental Implication

The riparian zone, a highly dynamic ecosystem, is the transitional region between land and river. Microplastics accumulation in riparian sediments has posed a potential ecosystem risk. However, the impact of MPs on riparian sediment structures and contaminant adsorption is still unclear. This study revealed that the sediment aggregate stability and DOM characteristics mediated by MPs were altered under different hydrological processes. Meanwhile, the adsorption of Cd(II) in sediments varied with microplastic concentrations and hydrological processes. Our results contribute to a better understanding of the ecological risks of MPs under different natural environments.

Declaration of Competing Interest

The authors declare that they have no known competing financial interests or personal relationships that could have appeared to influence the work reported in this paper.

Data Availability

The authors do not have permission to share data.

Acknowledgments

This study was supported by the Water Conservancy Science and Technology Project of Hunan Province (XSKJ2022068–20).

Appendix A. Supporting information

Supplementary data associated with this article can be found in the online version at doi:10.1016/j.jhazmat.2024.133589.

References

[1] He, W., Liu, S., Zhang, W., Yi, K., Zhang, C., Pang, H., Huang, D., Huang, J., Li, X., 2023. Recent advances on microplastic aging: Identification, mechanism, influence factors, and additives release. Sci Total Environ 889, 164035. https://doi.org/10.1016/j.scitotenv.2023.164035.

[2] Wazne, M., Mermillod-Blondin, F., Vallier, M., Hervant, F., Dumet, A., Nel, H.A., Kukkola, A., Krause, S., Simon, L., 2023. Microplastics in freshwater fediments impact the role of a main bioturbator in ecosystem functioning. Environ Sci Technol 57 (8), 3042–3052. https://doi.org/10.1021/acs.est.2c05662.

[3] Chen, M., Yang, D., Guo, F., Deng, R., Nie, W., Li, L., Yang, X., Liu, S., Chen, Y., 2023. Which sediment fraction mainly drives microplastics aging process: dissolved organic matter or colloids? J Hazard Mater 443, 130310. https://doi.org/10.1016/j.jhazmat.2022.130310.

[4] Wu, X., Liu, P., Zhao, X., Wang, J., Teng, M., Gao, S., 2022. Critical effect of biodegradation on long-term microplastic weathering in sediment environments: a systematic review. J Hazard Mater 437, 129287. https://doi.org/10.1016/j.jhazmat.2022.129287.

[5] Vandermeeren, P., Baken, S., Vanderstukken, R., Diels, J., Springael, D., 2016. Impact of dry-wet and freeze-thaw events on pesticide mineralizing populations and their activity in wetland ecosystems: a microcosm study. Chemosphere 146, 85–93. https://doi.org/10.1016/j.chemosphere.2015.11.089.

[6] Zhou, M., Li, Z., Huang, M., Ding, X., Wen, J., Wang, L., 2020. Impact of drying/wetting conditions on the binding characteristics of Cu(II) and Cd(II) with sediment dissolved organic matter. RSC Adv 10 (57), 34658–34669. https://doi.org/10.1039/d0ra04839a.

[7] Su, F., Li, Y., Qian, J., Zhang, Y., Wang, Y., Li, H., Li, M., 2022. Effect of repeated freezing–thawing on soil dissolved organic matter: a case study of brown farmland soil in Northeast China. Arab J Geosci 15 (24), 1754. https://doi.org/10.1007/s12517-022-11053-x.

[8] Wang, L., Zuo, X., Zheng, F., Wilson, G.V., Zhang, X.J., Wang, Y., Fu, H., 2020. The effects of freeze-thaw cycles at different initial soil water contents on soil erodibility in Chinese Mollisol region. Catena 193, 104615. https://doi.org/10.1016/j.catena.2020.104615.

[9] Nsabimana, G., Bao, Y., He, X., Nambajimana, Jd.D., Wang, M., Yang, L., Li, J., Zhang, S., Khurram, D., 2020. Impacts of water level fluctuations on soil aggregate stability in the three Gorges Reservoir, China. Sustainability 12 (21), 9107. https://doi.org/10.3390/su12219107.

[10] Liu, H., Xu, H., Wu, Y., Ai, Z., Zhang, J., Liu, G., Xue, S., 2021. Effects of natural vegetation restoration on dissolved organic matter (DOM) biodegradability and its temperature sensitivity. Water Res 191, 116792. https://doi.org/10.1016/j.watres.2020.116792.

[11] Chen, M., Hur, J., 2015. Pre-treatments, characteristics, and biogeochemical dynamics of dissolved organic matter in sediments: a review. Water Res 79, 10–25. https://doi.org/10.1016/j.watres.2015.04.018.

[12] Lee, Y.K., Murphy, K.R., Hur, J., 2020. Fluorescence signatures of dissolved organic matter leached from microplastics: polymers and additives. Environ Sci Technol 54 (19), 11905–11914. https://doi.org/10.1021/acs.est.0c00942.

[13] Liu, S., Huang, J., He, W., Zhang, W., Yi, K., Zhang, C., Pang, H., Huang, D., Zha, J., Ye, C., 2023. Impact of microplastics on lead-contaminated riverine sediments: based on the enzyme activities, DOM fractions, and bacterial community structure. J Hazard Mater 447, 130763. https://doi.org/10.1016/j.jhazmat.2023.130763.

[14] Sun, Y., Li, X., Li, X., Wang, J., 2022. Deciphering the fingerprint of dissolved organic matter in the soil amended with biodegradable and conventional microplastics based on optical and molecular signatures. Environ Sci Technol 56 (22), 15746–15759. https://doi.org/10.1021/acs.est.2c06258.

[15] Huang, M., Zhou, M., Li, Z., Ding, X., Wen, J., Jin, C., Wang, L., Xiao, L., Chen, J., 2022. How do drying-wetting cycles influence availability of heavy metals in sediment? A perspective from DOM molecular composition. Water Res 220, 118671. https://doi.org/10.1016/j.watres.2022.118671.

[16] Huang, J., Zhu, L., Zeng, G., Shi, L., Shi, Y., Yi, K., Li, X., 2019. Recovery of Cd(II) and surfactant in permeate from MEUF by foam fractionation with anionic-nonionic surfactant mixtures. Colloids Surf A: Physicochem Eng Asp 570, 81–88. https://doi.org/10.1016/j.colsurfa.2019.03.010.

[17] Shi, L., Huang, J., Zhu, L., Shi, Y., Yi, K., Li, X., 2019. Role of concentration polarization in cross flow micellar enhanced ultrafiltration of cadmium with low surfactant concentration. Chemosphere 237. https://doi.org/10.1016/j.chemosphere.2019.124859.

[18] Li, Y., Chen, M., Gong, J., Song, B., Shen, M., Zeng, G., 2021. Effects of virgin microplastics on the transport of Cd (II) in Xiangjiang River sediment. Chemosphere 283, 131197. https://doi.org/10.1016/j.chemosphere.2021.131197.

[19] Chen, L., Han, L., Feng, Y., He, J., Xing, B., 2022. Soil structures and immobilization of typical contaminants in soils in response to diverse microplastics. J Hazard Mater 438, 129555. https://doi.org/10.1016/j.jhazmat.2022.129555.

[20] Wang, Q., Sun, J., Yu, H., 2020. Impacts of different freeze-thaw treatments on the adsorption and desorption behaviors of Cd in black soil. Environ Sci Pollut Res 27 (10), 10990–10999. https://doi.org/10.1007/s11356-020-07709-4.

[21] Tang, S., Yang, X., Zhang, T., Qin, Y., Cao, C., Shi, H., Zhao, Y., 2022. Adsorption mechanisms of metal ions (Pb, Cd, Cu) onto polyamide 6 microplastics: new insight into environmental risks in comparison with natural media in different water matrices. Gondwana Res 110, 214–225. https://doi.org/10.1016/j.gr.2022.06.017.

[22] Sun, X., Tao, R., Xu, D., Qu, M., Zheng, M., Zhang, M., Mei, Y., 2023. Role of polyamide microplastic in altering microbial consortium and carbon and nitrogen cycles in a simulated agricultural soil microcosm. Chemosphere 312, 137155. https://doi.org/10.1016/j.chemosphere.2022.137155.

[23] Fuller, S., Gautam, A., 2016. A procedure for measuring microplastics using pressurized fluid extraction. Environ Sci Technol 50 (11), 5774–5780. https://doi.org/10.1021/acs.est.6b00816.

[24] Hale, S., Hanley, K., Lehmann, J., Zimmerman, A., Cornelissen, G., 2011. Effects of chemical, biological, and physical aging as well as soil addition on the sorption of pyrene to activated carbon and biochar. Environ Sci Technol 45 (24), 10445–10453. https://doi.org/10.1021/es202970x.

[25] Naisse, C., Girardin, C., Lefevre, R., Pozzi, A., Maas, R., Stark, A., Rumpel, C., 2015. Effect of physical weathering on the carbon sequestration potential of biochars and hydrochars in soil. GCB Bioenergy 7 (3), 488–496. https://doi.org/10.1111/gcbb.12158.

[26] Elliott, E.T., 1986. Aggregate structure and carbon, nitrogen, and phosphorus in native and cultivated soils. Soil Sci Soc Am J 50 (3), 627–633. https://doi.org/10.2136/sssaj1986.03615995005000030017x.

[27] Weishaar, J.L., Aiken, G.R., Bergamaschi, B.A., Fram, M.S., Fujii, R., Mopper, K., 2003. Evaluation of specific ultraviolet absorbance as an indicator of the chemical composition and reactivity of dissolved organic carbon. Environ Sci Technol 37, 4702–4708. https://doi.org/10.1021/es030360x.

[28] Maizel, A.C., Li, J., Remucal, C.K., 2017. Relationships between dissolved organic matter composition and photochemistry in lakes of diverse trophic status. Environ Sci Technol 51 (17), 9624–9632. https://doi.org/10.1021/acs.est.7b01270.

[29] Chen, W., Westerhoff, P., Leenheer, J.A., Booksh, K., 2003. Fluorescence excitation-emission matrix regional integration to quantify spectra for dissolved organic matter. Environ Sci Technol 37, 5701–5710.

[30] Han, L., Sun, K., Yang, Y., Xia, X., Li, F., Yang, Z., Xing, B., 2020. Biochar's stability and effect on the content, composition and turnover of soil organic carbon. Geoderma 364, 114184. https://doi.org/10.1016/j.geoderma.2020.114184.

[31] de Souza Machado, A.A., Lau, C.W., Till, J., Kloas, W., Lehmann, A., Becker, R., Rillig, M.C., 2018. Impacts of microplastics on the soil biophysical environment. Environ Sci Technol 52 (17), 9656–9665. https://doi.org/10.1021/acs.est.8b02212.

[32] Zhao, Z.Y., Wang, P.Y., Wang, Y.B., Zhou, R., Koskei, K., Munyasya, A.N., Liu, S.T., Wang, W., Su, Y.Z., Xiong, Y.C., 2021. Fate of plastic film residues in agro-ecosystem and its effects on aggregate-associated soil carbon and nitrogen stocks. J Hazard Mater 416, 125954. https://doi.org/10.1016/j.jhazmat.2021.125954.

[33] Li, G.Y., Fan, H.M., 2014. Effect of freeze-thaw on water stability of aggregates in a black soil of Northeast China. Pedosphere 24 (2), 285–290. https://doi.org/10.1016/s1002-0160(14)60015-1.

[34] Hu, B., Wang, Y., Wang, B., Wang, Y., Liu, C., Wang, C., 2018. Impact of drying-wetting cycles on the soil aggregate stability of Alfisols in southwestern China. J Soil Water Conserv 73 (4), 469–478. https://doi.org/10.2489/jswc.73.4.469.

[35] Utomo, W.H., Dexter, A.R., 1982. Changes in soil aggregate water stability induced by wetting and drying cycles in non-saturated soil. J Soil Sci 33 (4), 623–637. https://doi.org/10.1111/j.1365-2389.1982.tb01794.x.

[36] Oztas, T., Fayetorbay, F., 2003. Effect of freezing and thawing processes on soil aggregate stability. Catena 52 (1), 1–8. https://doi.org/10.1016/s0341-8162(02)00177-7.

[37] He, Z., Hou, R., Fu, Q., Li, T., Zhang, S., Su, A., 2023. Evolution mechanism of soil hydrothermal parameters under freeze–thaw cycles: regulatory significance of straw and biochar. J Clean Prod 385, 135787. https://doi.org/10.1016/j.jclepro.2022.135787.

[38] Zhao, T., Lozano, Y.M., Rillig, M.C., 2021. Microplastics increase soil pH and decrease microbial activities as a function of microplastic shape, polymer type, and exposure time. Front Environ Sci 9, 675803. https://doi.org/10.3389/fenvs.2021.675803.

[39] Yang, W., Cheng, P., Adams, C.A., Zhang, S., Sun, Y., Yu, H., Wang, F., 2021. Effects of microplastics on plant growth and arbuscular mycorrhizal fungal communities in a soil spiked with ZnO nanoparticles. Soil Biol Biochem 155, 108179. https://doi.org/10.1016/j.soilbio.2021.108179.

[40] Liu, Q., Huang, Y., Zhou, Y., Chen, Z., Luo, J., Yan, X., 2023. Impacts of wet-dry alternations on cadmium and zinc immobilisation in soil remediated with iron oxides. J Environ Manag 326, 116660. https://doi.org/10.1016/j.jenvman.2022.116660.

[41] Li, W., Wang, Z., Li, W., Li, Z., 2022. Impacts of microplastics addition on sediment environmental properties, enzymatic activities and bacterial diversity. Chemosphere 307, 135836. https://doi.org/10.1016/j.chemosphere.2022.135836.

[42] Han, Z., Deng, M., Yuan, A., Wang, J., Li, H., Ma, J., 2018. Vertical variation of a black soil's properties in response to freeze-thaw cycles and its links to shift of microbial community structure. Sci Total Environ 625, 106–113. https://doi.org/10.1016/j.scitotenv.2017.12.209.

[43] Bailey, V.L., Pries, C.H., Lajtha, K., 2019. What do we know about soil carbon destabilization? Environ Res Lett 14 (8), 083004. https://doi.org/10.1088/1748-9326/ab2c11.
[44] Shi, J., Wang, J., Lv, J., Wang, Z., Peng, Y., Shang, J., Wang, X., 2022. Microplastic additions alter soil organic matter stability and bacterial community under varying temperature in two contrasting soils. Sci Total Environ 838, 156471. https://doi.org/10.1016/j.scitotenv.2022.156471.
[45] Qi, Y., Beriot, N., Gort, G., Huerta Lwanga, E., Gooren, H., Yang, X., Geissen, V., 2020. Impact of plastic mulch film debris on soil physicochemical and hydrological properties. Environ Pollut 266, 115097. https://doi.org/10.1016/j.envpol.2020.115097.
[46] Bongiorno, G., Bünemann, E.K., Oguejiofor, C.U., Meier, J., Gort, G., Comans, R., Mäder, P., Brussaard, L., de Goede, R., 2019. Sensitivity of labile carbon fractions to tillage and organic matter management and their potential as comprehensive soil quality indicators across pedoclimatic conditions in Europe. Ecol Indic 99, 38–50. https://doi.org/10.1016/j.ecolind.2018.12.008.
[47] Chen, M., Liu, S., Bi, M., Yang, X., Deng, R., Chen, Y., 2022. Aging behavior of microplastics affected DOM in riparian sediments: from the characteristics to bioavailability. J Hazard Mater 431, 128522. https://doi.org/10.1016/j.jhazmat.2022.128522.
[48] Tsai, K.P., Chow, A.T., 2016. Growing algae alter spectroscopic characteristics and chlorine reactivity of dissolved organic matter from thermally-altered forest litters. Environ Sci Technol 50 (15), 7991–8000. https://doi.org/10.1021/acs.est.6b01578.
[49] Huang, J., Yang, Y., Zeng, G., Gu, Y., Shi, Y., Yi, K., Ouyang, Y., Hu, J., Shi, L., 2019. Membrane layers intensifying quorum quenching alginate cores and its potential for membrane biofouling control. Bioresour Technol 279, 195–201. https://doi.org/10.1016/j.biortech.2019.01.134.
[50] Liu, Z., Pang, H., Yi, K., Wang, X., Zhang, W., Zhang, C., Liu, S., Gu, Y., Huang, J., Shi, L., 2024. Isolation and application of *Bacillus thuringiensis* LZX01: Efficient membrane biofouling mitigation function and anti-toxicity potential. Bioresour Technol 394, 130272. https://doi.org/10.1016/j.biortech.2023.130272.
[51] Leenheer, J.A., Wershaw, R.L., Brown, G.K., Reddy, M.M., 2003. Characterization and diagenesis of strong-acid carboxyl groups in humic substances. Appl Geochem 18, 471–482. https://doi.org/10.1016/S0883-2927(02)00100-2.
[52] McKnight, D.M., Boyer, E.W., Westerhoff, P.K., Doran, P.T., Kulbe, T., Andersen, D.T., 2001. Spectrofluorometric characterization of dissolved organic matter for indication of precursor organic material and aromaticity. Limnol Oceanogr 46 (1), 38–48. https://doi.org/10.4319/lo.2001.46.1.0038.
[53] Garcia, R.D., Diéguez, Md.C., Gerea, M., Garcia, P.E., Reissig, M., 2018. Characterisation and reactivity continuum of dissolved organic matter in forested headwater catchments of Andean Patagonia. Freshw Biol 63, 1049–1062. https://doi.org/10.1111/fwb.13114.
[54] Shutova, Y., Baker, A., Bridgeman, J., Henderson, R.K., 2014. Spectroscopic characterisation of dissolved organic matter changes in drinking water treatment: From PARAFAC analysis to online monitoring wavelengths. Water Res 54, 159–169. https://doi.org/10.1016/j.watres.2014.01.053.
[55] Murphy, K.R., Hambly, A., Singh, S., Henderson, R.K., Baker, A., Stuetz, R., Khan, S.J., 2011. Organic matter fluorescence in municipal water recycling schemes: toward a unified PARAFAC model. Environ Sci Technol 45 (7), 2909–2916. https://doi.org/10.1021/es103015e.
[56] Yamashita, Y., Boyer, J.N., Jaffé, R., 2013. Evaluating the distribution of terrestrial dissolved organic matter in a complex coastal ecosystem using fluorescence spectroscopy. Cont Shelf Res 66, 136–144. https://doi.org/10.1016/j.csr.2013.06.010.
[57] Pallem, V.L., Stretz, H.A., Wells, M.J.M., 2009. Evaluating aggregation of gold nanoparticles and humic substances using fluorescence spectroscopy. Environ Sci Technol 43, 7531–7535. https://doi.org/10.1021/es901201z.
[58] Li, Z., Huang, M., Luo, N., Wen, J., Deng, C., Yang, R., 2019. Spectroscopic study of the effects of dissolved organic matter compositional changes on availability of cadmium in paddy soil under different water management practices. Chemosphere 225, 414–423. https://doi.org/10.1016/j.chemosphere.2019.03.059.
[59] Liu, S., Huang, J., Zhang, W., Shi, L., Yi, K., Zhang, C., Pang, H., Li, J., Li, S., 2022. Investigation of the adsorption behavior of Pb(II) onto natural-aged microplastics as affected by salt ions. J Hazard Mater 431, 128643. https://doi.org/10.1016/j.jhazmat.2022.128643.
[60] Shi, L., Huang, J., Zeng, G., Zhu, L., Gu, Y., Shi, Y., Yi, K., Li, X., 2019. Roles of surfactants in pressure-driven membrane separation processes: a review. Environ Sci Pollut Res 26 (30), 30731–30754. https://doi.org/10.1007/s11356-019-06345-x.
[61] Huang, B., Li, Z., Huang, J., Guo, L., Nie, X., Wang, Y., Zhang, Y., Zeng, G., 2014. Adsorption characteristics of Cu and Zn onto various size fractions of aggregates from red paddy soil. J Hazard Mater 264, 176–183. https://doi.org/10.1016/j.jhazmat.2013.10.074.
[62] Guan, Y., Gong, J., Song, B., Li, J., Fang, S., Tang, S., Cao, W., Li, Y., Chen, Z., Ye, J., Cai, Z., 2022. The effect of UV exposure on conventional and degradable microplastics adsorption for Pb (II) in sediment. Chemosphere 286, 131777. https://doi.org/10.1016/j.chemosphere.2021.131777.
[63] Li, X.Y., Lin, J.Y., Zhang, J., Liu, H.T., 2023. Response of occurrence in microplastics and its adsorped cadmium capacity to simulated agricultural environmental scenarios in sludge-amended soil. Environ Res 222, 115346. https://doi.org/10.1016/j.envres.2023.115346.
[64] Liu, J., Li, Y., Wang, Y., Wang, Y., Xu, J., Liu, X., 2023. Competitive adsorption of lead and cadmium on soil aggregate at micro-interfaces: multi-surface modeling and spectroscopic studies. J Hazard Mater 448, 130915. https://doi.org/10.1016/j.jhazmat.2023.130915.
[65] Jin, C., Li, Z., Huang, M., Wen, J., Ding, X., Zhou, M., Cai, C., 2021. Laboratory and simulation study on the Cd(II) adsorption by lake sediment: Mechanism and influencing factors. Environ Res 197, 111138. https://doi.org/10.1016/j.envres.2021.111138.
[66] Tang, S., Lin, L., Wang, X., Sun, X., Yu, A., 2021. Adsorption of fulvic acid onto polyamide 6 microplastics: Influencing factors, kinetics modeling, site energy distribution and interaction mechanisms. Chemosphere 272, 129638. https://doi.org/10.1016/j.chemosphere.2021.129638.
[67] Huang, L., Jin, Q., Tandon, P., Li, A., Shan, A., Du, J., 2018. High-resolution insight into the competitive adsorption of heavy metals on natural sediment by site energy distribution. Chemosphere 197, 411–419. https://doi.org/10.1016/j.chemosphere.2018.01.056.
[68] Liu, C., Li, Z., Berhe, A.A., Xiao, H., Liu, L., Wang, D., Peng, H., Zeng, G., 2019. Characterizing dissolved organic matter in eroded sediments from a loess hilly catchment using fluorescence EEM-PARAFAC and UV–visible absorption: Insights from source identification and carbon cycling. Geoderma 334, 37–48. https://doi.org/10.1016/j.geoderma.2018.07.029.
[69] Yan, L., Xie, X., Heiss, J.W., Peng, K., Deng, Y., Gan, Y., Li, Q., Zhang, Y., 2023. Isotopic and spectral signatures unravel the sources, preservation and degradation of sedimentary organic matter in the Dongzhai Harbor mangrove estuary, southern China. J Hydrol 618, 129256. https://doi.org/10.1016/j.jhydrol.2023.129256.
[70] Zhu, K., Li, W., Yang, S., Ran, Y., Lei, X., Ma, M., Wu, S., Huang, P., 2022. Intense wet-dry cycles weakened the carbon sequestration of soil aggregates in the riparian zone. Catena 212, 106117. https://doi.org/10.1016/j.catena.2022.106117.